Research article

Title:

Arabinogalactan proteins mediate intercellular crosstalk in the ovule of apple flowers

Juan M. Losada[1,2,3*]

María Herrero[1]

[1]Pomology Department, Aula Dei Experimental Station-CSIC. Avda Montañana 1005. Zaragoza, Spain, 50059.

[2]Arnold Arboretum of Harvard University. 1300 Centre St. Boston, MA, 02131.

[3]Instituto de Hortofruticultura Subtropical y Mediterránea La Mayora-CSIC-UMA. Avda. Dr. Wienberg s/n. Algarrobo-Costa, Málaga, Spain, 29750.

Key Message: AGP-rich glycoproteins mediate pollen-ovule interactions and cell patterning in the embryo sac of apple before and after fertilization**.**

*E-mail address: juan.losada@csic.es

Abstract

Glycoproteins are significant players in the dialog that takes place between growing pollen tubes and the stigma and style in the angiosperms. Yet, information is scarce on their possible involvement in the ovule, a sporophytic organ that hosts the female gametophyte. Apple flowers have a prolonged lapse of time between pollination and fertilisation, offering a great system to study the developmental basis of glycoprotein secretion and their putative role during the last stages of the progamic phase and early seed initiation. For this purpose, the sequential pollen tube elongation within the ovary was examined in relation to changes in arabinogalactan proteins (AGPs) in the tissues of the ovule before and after fertilization. To evaluate what of these changes are developmentally regulated, unpollinated and pollinated flowers were compared. AGPs paved the pollen tube pathway in the ovules along the micropylar canal, and the nucellus entrance towards the synergids, which also developmentally accumulated AGPs at the filiform apparatus. Glycoproteins vanished from all these tissues following pollen tube passage, strongly suggesting a role in pollen-ovule interaction. In addition, AGPs marked the primary cell walls of the haploid cells of the female gametophyte, and they further built up in the cell walls of the embryo sac and developing embryo, layering the interactive walls of the three generations hosted in the ovule, the maternal sporophytitic tissues, the female gametophyte, and the developing embryo.

Key words: Arabinogalactan proteins **(**AGPs), apple, embryo sac, *Malus* x *domestica*, ovule, pollen tube.

Introduction

Regardless of the ubiquity of double fertilization in flowering plants, the intimate male-female cross talk that takes place during the transition between the haploid and diploid generations appears to be species specific. The structural complexity of the angiosperm ovules (Endress 2011), protected within the gynoecium, and the lack of well-described stages of pollen tube growth in the ovules of many flowering plants, made most works focused on pollen tube-ovule interactions in model species (reviewed by Lora et al. 2016; Kanaoka 2018; Li et al. 2018). Yet, detection of the factors involved in non-model species is essential to understand homologous players during pre- and post- fertilization events across taxa (Gibbs 2014).

The female gametophyte is nested in the nucellus, which is wrapped by the integuments forming the ovules, stalked in the ovary with a funiculus (Bouman 1984; Endress 2011). The role of sporophytic tissues of the ovules on gametophyte protection pairs with physical and chemical guidance of pollen tubes towards the female gametophyte (Hülskamp et al. 1995; Herrero 2000, 2001; Johnson and Preuss 2002; Kessler and Grosniklaus 2011). Physically, the corridor between the integuments (i.e. micropyle) marks the area through which pollen tubes elongate before entering the nucellus (Hofmeister 1849; Dresselhaus and Márton 2009; Lora et al. 2018). The style provides sugar-rich compounds that nurture the elongating pollen tubes (Herrero and Dickinson 1979, 1981). Once in the ovary, coordination of exudates from the sporophytic tissues and pollen tube elongation appears to be a prerequisite for a successful fertilization (Herrero 2003).

The entrance of pollen tubes into the female gametophyte occurs invariably through the synergids, located at the micropylar-most pole (Punwani and Drews 2008; Leshem et al. 2013). Synergids have highly convoluted secretory cell walls at their micropylar side, known as the filiform apparatus, which have been related with secretion of diffusible molecules that attract pollen tubes in model species (Higashiyama et al. 2001; Sandaklie-Nikolova et al. 2007; Punwani et al. 2007; Dresselhaus et al. 2016). In *Arabidopsis*, mutants lacking the filiform apparatus and their secretions result in failure of sperm discharge by pollen tubes (Kasahara et al. 2005; Punwani and Drews 2008). Similar factors in maize -ZmEA1 factor- are also involved

in short range pollen tube attraction before fertilisation (Márton et al. 2005; 2012; Okuda et al. 2009; Márton and Dresselhaus 2010). How far these signals can reach is still under debate, but in the genus *Torenia*, where the synergids are unprotected, small proteins have been described as pollen tube attractants both *in vivo* and *in vitro* (Higashiyama and Hamamura 2008; Sankaranarayanan and Higashiyama 2018). More recently, a critical role of arabinogalactan proteins from the gynoecial tissues in pollen tube performance before fertilization was described in *Torenia* flowers (Mizukami et al. 2016; Mizuta and Higashiyama 2018; Su and Higashiyama 2018). This is in line with the increasing evidence that AGPs are ubiquitous players during male-female interactions in flowering plants (reviewed by Pereira et al. 2015, 2016; Leszczuk et al. 2019b). AGP epitopes recognised through immunolocalization have been described in the ovules of unrelated angiosperm genera such as in *Actinidia*, *Amaranthus* (Coimbra and Salema 1997; Coimbra and Duarte 2003), *Brassica* (Pennel et al. 1991), *Arabidopsis* (Coimbra et al. 2007; Lora et al. 2018), *Pitcairnia* (Mendes et al. 2014), *Quercus* (Lopes et al. 2016; Costa et al. 2017), *Taraxacum* (Gawecki et al. 2017), *Annona* (Lora et al. 2018), or *Fragaria* (Leszczuk and Szczuka 2018; Leszczuk et al. 2019a, c). Among all the available works, change in AGPs of the ovules after pollen tube growth has been overlooked, an observation that is key to understand a possible interactive relationship between the ovular tissues and the elongating pollen tubes.

During the last few years, the progamic phase of apple flowers helped to better understand the role of glycoproteins during the communication between the pollen tubes and the sporophytic tissues of the gynoecium. Using immunolocalization techniques combined with pollination experiments in the field, we reported that a timely secretion of different glycoproteins (mainly AGPs and extensins), along the gynoecium of apples in concomitance with pollen tube elongation, first on the stigma (Losada and Herrero 2012), then in the style (Losada and Herrero 2014), and on the obturator (Losada and Herrero 2017). These results supported a synchrony between maturation of these tissues, marked by a secretory phase, and the elongation of the pollen tubes. The need for male-female synchrony has further been put forward also in the ovary (Herrero 2003), and indeed secretion time is responsible for pollen tube behaviour in the ovule

(Herrero 2000, 2001), but the nature of this secretion is unknown. This work evaluates the possible role of arabinogalactan proteins as mediators of male-female dialog in the ovule of apple flowers.

Materials and methods

Plant material

Flowers from apple trees cv Golden Delicious Spur grown in the province of Huesca (Northeast Spain) were used. Since apple flowers are self-incompatible, the compatible cv Royal Gala was used as the pollen donor. Thus, 100 flowers from cv Royal Gala were collected before pollen release, anthers dissected and left to dry on paper at room temperature (approximately 20ºC), for 24-48 h until dehiscence. Then, anthers were sieved with a metallic mesh with a pore diameter of 0.26 mm, and the sieved pollen was used to hand pollinate 50 flowers of the cv Golden Delicious, which were previously emasculated the day before petal opening to avoid pollen contamination from other sources. As negative controls, 50 flowers were emasculated before petal opening and left unpollinated.

Pollen tube growth in the ovary

Following hand pollination, three flowers were collected every day for a period of ten days. Flowers were fixed in formalin: acetic acid: alcohol 70%-FAA (1:1:18) (Johansen 1940) for 24 h. To evaluate pollen tube elongation with time, the hypanthium of flowers from all post pollination stages was dissected, washed in distilled water, and later dehydrated in a series of increasing concentrations of tertiary butyl alcohol (TBA) (50%, 70%, 85%, 95%, 100% trice), for 3 h in each. Hypanthia were incubated in TBA: paraffin oil (1:1) overnight, and infiltrated in paraffin-paraplast wax at 60ºC for one month. Finally, paraffin blocks containing the samples were hardened, and serially sectioned, at 10µm thickness, with a Leica Jung 2045 rotatory microtome (Leica Microsystems S.L.U., Barcelona, Spain).

Sections were placed onto glass slides previously coated with Haupt´s adhesive (filtered from a mixture of 1g of gelatine in 100mL of water, 2g of phenol crystals, and 15mL glycerin), and deparaffinised with a

series of decreasing concentrations of Histoclear: ethanol starting from 100% Histoclear, and going through 70%, 50%, 20% (v/v) concentrations. Then, the sections were hydrated in distilled water three times, 5 min each, and stained with 0.1% aniline blue in 0.1 N K_3PO_4 to visualize pollen tubes (Linskens and Esser 1957). Pollen tube tip arrival to the funiculus, obturator, micropyle, nucellus and embryo sac was timed. Each flower has five locules, with two ovules per locule, resulting in 10 ovules per flower, and 30 ovules per sample point. After hand pollinations, five extra flowers from the tenth day after pollination (receptacle enlarged) were used to observe the localization of the pollen tubes in the ovules. Flowers were water-washed, placed in 5 % sodium sulphite for 24 h, autoclaved for 10 min at 1 kg cm−2 (Jefferies and Belcher, 1974), and squashed onto glass slides with 0·1 % aniline blue in 0.1 n K3PO4 to visualize pollen tubes (Linskens and Esser 1957). Pollen tubes were observed with a LEICA DM2500 fluorescence microscope using a 340/400 nm filter, and images obtained with a CANON Power Shot S50 camera linked to the CANON Remote Capture software.

Sample preparation for examination of ovule anatomy

Three pollinated and three unpollinated flowers (n=60 ovules) were collected per day at anthesis, five, six, eight and ten days after pollination, or five, six, eight and ten days after anthesis for unpollinated flowers. Receptacles from these flowers were fixed in a solution of 4% paraformaldehyde in 1M phosphate buffered saline (PBS), pH 7.3 overnight, washed in 1M PBS to remove the fixative, and then dehydrated through a series of increasing acetone concentrations (10%, 20%, 35%, 50%, 70%, 80%, 100%), 1 h each. Later, the ovaries were infiltrated with the Technovit 8100 glycol methacrylate resin (Electron Microscopy Sciences, Hatfield, PA, USA), and hardened at 4°C under anoxic conditions. Blocks were sectioned at 2µm using a LEICA EM UC6 ultramicrotome with a glass knife (Leica Microsystems, S.L.U., Barcelona, Spain), placed in a drop of water on a slide previously coated with 2% (3-Aminopropyl) triethoxysilane (Merck KGaA, Darmstadt, Germany) (Solís et al. 2008). Sections were stained with periodic acid shift reagent-PAS (Feder and O´Brien 1968) that stains insoluble polysaccharides, and some of the sections counterstained

with a 0.02% aqueous solution of Toluidine Blue. Slides were observed under a Zeiss Axio Imager Z2 microscope equipped with a Zeiss HR Axiocam digital camera (Zeiss, Oberkochen, Germany).

Glycoprotein epitope detection in the ovules

To test for the presence of arabinogalactan proteins (AGPs), ovules were freshly dissected with the integuments, or further dissecting the integuments to expose the nucellus, and placed in an 0.15M NaCl solution containing 2mg of the chemical agent beta-glucosyl Yariv reagent (β-Glc-YR) (Biosupplies, Victoria, Australia), which gives a red colour when AGPs precipitate, while the alpha-galactosyl Yariv reagent (α-Gal-YR) was used as a negative control (Yariv et al. 1967). The positive results of this test led to the immunodetection of AGP glycan epitopes in the ovular tissues.

AGPs were also detected with two monoclonal antibodies that previously revealed their localization along the pollen tube pathway of apple styles (Losada and Herrero 2017). These were two anti-rat primary monoclonal antibodies (MAbs), JIM8 (Pennell et al. 1991), and JIM13 (Knox et al. 1991) (Carbosource Services, Atlanta, Georgia, USA). For this purpose 2μm sections, of Technovit 8100 embedded samples, were incubated in 1M PBS for 5 min, then with 5% w/v bovine serum albumin (BSA) in PBS for 5 min, and later with the primary antibodies for 1 h. After that, samples were washed thrice in PBS 5 min each, and incubated with an anti-rat Alexa 488 fluorochrome (Thermo Fisher, Waltham, Massachusetts, USA), for 45 min in the dark. Finally, following three washes in PBS, the sections were counterstained either with calcofluor white that detects cellulose and pectins in the cell walls (Hughes and McCully 1975), or with 0.1 mg/mL aqueous 4,6-Diamidino-2-phenylindole (DAPI) to visualize DNA in the nucleus. All slides were mounted in ProLong Gold Antifade reagent (Thermo Fisher) and examined with a Leica DM LB2 epifluorescence microscope equipped with a Leica DFC310 FX camera, which is connected to a Leica Acquisition Station AF6000 E software. Filters for calcofluor white, and DAPI staining were 355/455 nm; and 470/525 nm for the Alexa 488 fluorescein label of the antibodies (White Level = 255; Black Level = 0; ϒ = 1).

Results

Dynamic observation of pollen tube growth in the ovary

In apple flowers, the progamic phase that goes from pollination to fertilization (Linskens 1975), lasted for one week (Losada and Herrero 2017). Pollen tubes reached the base of the style the third day after pollination (Losada and Herrero 2014), and started to be observed in most ovules at the funiculus (Fig. 1). The first pollen tubes reached the obturator surface four days after pollination, and faced the ovule, where the pollen tube traversed two sporophytic domains: the micropyle, flanked by the outer and the inner integuments (Fig. 2a), and the nucellus (Fig. 2b). While most obturators were traversed by pollen tubes, only 60% of the ovules evaluated showed pollen tubes in the micropyle and in the nucellus (Fig 1), six to seven days after pollination, when fertilization occurred.

Arabinogalactan proteins in the ovules before fertilization

Preliminary tests for arabinogalactan proteins with the biochemical reagent Yariv revealed secretions rich in AGPs exudated from the micropyle (Fig. 3a-c), and from the nucellus (Fig. 3e-g) before pollen tube arrival, but correlated with the areas of pollen tube elongation toward the female gametophyte (Fig. 3d, h). Immunolocalization of arabinogalactan protein epitopes confirmed these observations, and revealed that secretions rich in AGPs epitopes were particularly abundant along the pollen tube pathway in the sporophytic areas of the ovule. Consistent with Yariv labelling, cells at the micropylar tip of the nucellus also exuded AGPs labeled by JIM13 at anthesis (Fig. 4a-c). Six days later, concomitantly with pollen tube arrival to the micropyle (Fig. 4d), AGPs labeled with JIM13 were secreted to the micropylar canal, and contacted the elongating pollen tubes (Fig. 4e,f). Strinkingly, as the pollen tube arrived to the nucellus (Fig. 4g), the exudate rich in AGPs weakened from the area between the nucellus and the integuments (Fig. 4h,i). Furthermore, in the nucellus, a very specific row of cells leading to the synergids marked the area of pollen tube penetration, and this ‘trail’ was labeled with both JIM8 (Fig. 5a), as well as

with JIM13 (Supplementary Fig. 1a) AGP epitopes at anthesis. However, following pollen tube passage, epitopes vanished from this area (Fig. 5b; Supplementary Fig. 1b). This idea is reinforced by their accumulation in the nucellus of unpollinated ovules (Fig. 5c).

Arabinogalactan proteins in the embryo sac

At anthesis, some ovules were still immature, but most ovules had a fully developed Polygonum type female gametophyte, showing two unfused polar nuclei in a large central cell, two synergids, and the egg cell at the micropylar side (Fig. 6a), and three antipodals at the chalazal-most pole. During the post pollination stages, the central cell accumulated starch grains (Fig 6b; Supplementary Fig. 2a). Unfertilized female gametophytes, showed a more disorganized structure, with polar nuclei fused, and a number of globular vesicles that did not stain for insoluble polysaccharides (Fig. 6c). After fertilization, elongation of the embryo sac was concomitant with proliferation of a syncytial endosperm (Fig. 6d). The filiform apparatus of the synergids showed convoluted cell walls that accumulated polysaccharides from anthesis (Fig. 6e) through the post pollination stages, upon pollen tube arrival, when one synergid degenerated (Fig 6f; Supplementary Fig. 2b). While unfertilized ovules also had a conspicuous polysaccharide labelling in the filiform apparatus (Fig. 6g), fertilized ovules showed a collapsed filiform apparatus (Fig. 6h; Supplementary Fig. 2c).

At anthesis, the highly folded walls of the central cell as well as the walls separating the cells of the egg apparatus - the egg cell plus two synergids - did not stain for cellulose, but were labeled for AGP epitopes recognized by JIM8 (not shown), and JIM13mAb (Figs. 7a, b, c). Six days after pollination, upon penetration of the pollen tube in the nucellus, the walls of egg cell and central cell further labeled for AGPs, as well as some vesicles (Figs. 7d, e, f). Unfertilized gametophytes kept this labeling, as well as in numerous vesicles in the central cell (Fig. 7g, h, i). A close look at the filiform apparatus showed that, among all the haploid cells in the female gametophyte, only the convoluted walls of the filiform apparatus showed noticeable cellulose staining (Fig. 8a). Interestingly, the tips of these cell wall invaginations displayed AGPs soon after pollination (Fig. 8b, c). These AGP epitopes continued to accumulate in the

filiform apparatus, and at the time of pollen tube arrival, they pervaded its convoluted wall structure (Fig. 8d, e, f). Following fertilization, AGPs vanished as the filiform apparatus degenerated (Fig. 8g, h, i), but a remarkable presence of AGP epitopes could be detected in the primary wall of the zygote (Fig. 8h, i), as well as in the primary walls of the young embryo (Fig. 8j, k, l).

Discussion

Arabinogalactan proteins paved the pollen tube pathway in the ovule, and vanished after pollen tube passage. AGPs also layered the primary cell walls of the embryo sac and, following fertilization, of the young embryo (Fig. 9).

AGPS pave the micropyle and nucellar tip and interact with the pollen tube

The pollen tube slows down in the ovary of the apple flower, as compared with the rapid elongation in the stylar transmitting tract (Losada and Herrero 2014). This slowdown has also been reported in peach (Arbeloa and Herrero 1987), where it is related to a delay in development of the pistil structures the pollen tube has to traverse (Herrero and Arbeloa 1989). In peach, the ovule is orthotropous, with the micropyle facing the base of the style, and thus pollen tubes have a putative direct access to the ovules. Conversely, in apple flowers, the ovules are anatropous, bending down with the micropyle facing down the placenta, and the pollen tube needs to traverse a longer distance through the funiculus, and finally switching the elongating tip towards the ovule entrance (Losada and Herrero 2017). Prolonging the distance required to undergo fertilization may be a mechanism to guarantee male-female synchrony that is a prerequisite for a successful mating (Herrero 2003). In spite of these physical restrictions, exudation of AGPs in the micropyle and nucellus occurs way before pollen tube arrival, suggesting that they accumulate a secretion that pave the pollen tube pathway before fertilization, marking the areas of pollen tube entrance toward the female gametophyte.

AGPs have been immunolabeled in the micropyle and/or nucellus of a handful of angiosperm species prior to pollen tube arrival, including *Actinidia deliciosa*, *Amaranthus hypochondriacus* (Coimbra and Duarte 2003), *Taraxacum officinalis* (Gawecki et al. 2017), *Olea europaea* (Suárez et al. 2013), *Arabidopsis thaliana* (Coimbra et al. 2007; Lora et al. 2018), *Annona cherimola* (Lora et al. 2018), *Quercus suber* (Costa et al. 2017), or *Fragaria* x *ananassa* (Leszczuk and Szczuka 2018; Leszczuk et al. 2019a, c). This consistent presence in different species contrasts with the paucity of information on their implications on pollen-ovule interaction. Results herein, in apple flowers, show that AGPs both in the micropylar canal and in the nucellar tip deplete following pollen tube passage. This suggests the provision of an adequate media for pollen tube growth with a nutritional role during the last steps of the progamic phase, similar to previous observations in the stigma, style and obturator (Losada and Herrero 2012, 2014, 2017), and concordant with previous observations of heterotrophic pollen tube growth (Herrero and Dickinson 1979, 1981). But the presence of AGPS along the pollen tube pathway does not seem restricted to the sporophytic domain, for it seems to be also present in the female gametophyte.

AGPs accumulate in the filiform apparatus of the synergids and vanish upon pollen tube penetration

The first contact between pollen tubes and the female gametophyte occurs in the synergids. In apple, the filiform apparatus of the synergids is quite developed and contain polysaccharides at anthesis. The cumulative presence of polysaccharides in the filiform apparatus during the time of the progamic phase (five to six days), concord with immunolocalization of AGP epitopes, which developmentally accumulated in the filiform apparatus from anthesis to six days later, when pollen tubes arrive at the female gametophyte. The presence of AGPs in the convoluted filiform apparatus is quite conspicuous in the angiosperm species where it has been investigated, including *Pitcairnia encholirioides* (Mendes et al. 2014), *Brassica napus* (Pennell et al. 1991), *Taraxacum officinalis* (Gawecki et al. 2017), *Arabidopsis thaliana* (Coimbra et al. 2007), and *Quercus suber* (Lopes et al. 2016; Costa et al. 2017). Our work further reveals depletion of both polysaccharides and AGP epitopes from the filiform apparatus of the synergids after fertilization, whereas

they hyper-accumulated in the filiform apparatus of unfertilized ovules. This suggests that AGPs from the filiform apparatus are involved in the nutrition-guidance of pollen tubes prior to fertilization.

Similarly, recent works in model species showed the direct involvement of AGPs derived from the synergids on pollen tube capacitance in *Torenia* (Mizukami et al. 2016; Sankaranarayanan and Higashiyama 2018), as well as preventing polytubey in *Arabidopsis* (Pereira et al. 2016). Interestingly, the elongating wall of the male gametophyte uses AGPs among other compounds as building blocks, described in a number of angiosperm species with different evolutionary histories [*Annona cherimola* and *Asimina triloba* (Mollet et al. 2002; Losada et al. 2017), *Lilium longiflorum* (Jauh and Lord 1996), *Nicotiana tabacum* (Qin et al. 2007; Derksen et al. 2011), *Arabidopsis thaliana* (Dardelle et al. 2010; Nguema-Ona et al. 2012; Pereira et al. 2006, 2014), *Actinidia chinensis* (Speranza et al. 2009), *Olea europaea* (Suárez et al. 2013; Castro et al. 2013)]. As a result, AGPs provided by the micropyle and nucellus may likely serve as the nutritional molecules for male gametophyte nutrition -and orientation- before syngamy, but those of the filiform apparatus may also facilitate pollen tube discharge within the synergids.

Plastic walls and the transition among generations

In the majority of ovules observed, the apple female gametophyte is completely cellularized at anthesis, concordant with previous observations in apple (Costa Tura and Mackenzie 1990), and changes in its structure occur during the seven days that pollen tubes take to arrive to this structure, such as vacuolization of the central cell, synergids and the egg cell, and starch accumulation. In unpollinated flowers, female gametophytes showed a chaotically arranged structure seven days after anthesis - the time of the progamic phase in pollinated flowers. This suggests that pollination triggers a prolongation of embryo sac viability, as previously reported in pear flowers (Herrero and Gascón 1987). In this species this prolongation of embryo sac viability is also mimicked by treatment with gibberellic acid. Conversely a too young female gametophyte at the time of pollen tube arrival may also jeopardise fertilization, and thus, delays in female gametophyte maturation cause pollen tube stagnation in the ovaries (Sogo and Tobe 2006, 2008; Liu et al. 2014). All this support the idea that a fully developed female gametophyte (i.e. cellularized)

at the time of pollen tube arrival is a prerequisite for a timely fertilization (Herrero 2003), and AGPs appear to play a critical role on separating this complex group of haploid cells.

A handful of previous studies reported localization of AGPs separating the megagametophyte cells, such as in *Pitcairnia encholirioides* (Mendes *et al*. 2014), *Arabidopsis* (Coimbra et al. 2007; Lopes et al. 2016; Lora et al. 2018), and *Quercus* (Lopes et al. 2016). Our work confirms that the primary walls separating the haploid cells of the apple female gametophyte are labelled with AGP epitopes. They are also present, after fertilization in the young apple embryo walls, as it has also been reported in other species (Pennell et al. 1991; Vaughn et al. 2007; Zhong et al. 2011; Lopes et al. 2016), supporting their role in embryogenesis (Pérez-Pérez et al., 2019). Moreover, they appear to be pre-designed for the rapid elongation of the embryo sac following fertilization, as shown by the accumulation of vesicles rich in AGPs in unfertilized gametophytes. The ubiquitous presence of AGPs in plant cell primary walls has been related with cell volumetric changes (Dardelle et al. 2010), or wall flexibility (Moore et al. 2013), and could provide plasticity enabling relatively rapid changes during the transition among generations, as it occurs not only in angiosperms, but also (Lopez and Renzaglia 2016) in other vascular plants.

Conclusions

Results from this work show the presence of AGPs in the boundaries of the different individuals that share hosting within an ovule: the sporophytic tissues of the ovule, the advancing male gametophyte, the secluded female gametophyte, and later on the young embryo. But the role of AGPs in the ovule before fertilization, paving the pollen tube pathway and vanishing following pollen tube passage, goes beyond physical properties, strongly suggesting a role in male-female interaction with a common language shared by the female sporophyte and the female gametophyte that seems to be well understood by the male gametophyte.

Acknowledgements

Authors are grateful to Reyes Lopez for technical assistance, and Nuria Blanco-Moure for helping with graphs and data analysis. We thank William E. Friedman for his support and for providing lab equipment during part of this work. This work was supported by Ministerio de Ciencia e Innovación (MICINN)-FEDER [AGL2006-13529-C02-01, AGL 12621-C02-01, AGL 2012–40239], and Gobierno de Aragón [group A43]. JIM antibodies distribution was partly supported by NSF grants [DBI-0421683, RCN 009281]. J.M.L. was supported by a FPI fellowship [BES-2007-16059] from MICINN.

Compliance with ethical standards

Conflict of interest. The authors declare that they have no conflict of interest.

References

Arbeloa A, Herrero M (1987) The significance of the obturator in the control of pollen tube entry into the ovary in peach (*Prunus persica*). Ann Bot 60: 681–685. https://doi.org/10.1093/oxfordjournals.aob.a087500.

Bouman F. 1984. The ovule. In: Johri BM (ed) Embryology of angiosperms. Berlin: Springer pp, 123–157.

Castro AJ, Suárez C, Zienkiewicz K, de Dios Alché J, Zienkiewicz A, Rodríguez-García MI (2013) Electrophoretic profiling and immunocytochemical detection of pectins and arabinogalactan proteins in olive pollen during germination and pollen tube growth. Ann Bot 112: 503–513. https://doi.org/10.1093/aob/mct118.

Coimbra S, Almeida J, Junqueira V, Costa ML, Pereira LG (2007) Arabinogalactan proteins as molecular markers in *Arabidopsis thaliana* sexual reproduction. J Exp Bot 58: 4027–4035. https://doi.org/10.1093/jxb/erm259.

Coimbra S, Duarte C (2003) Arabinogalactan proteins may facilitate the movement of pollen tubes from the stigma to the ovules in *Actinidia deliciosa* and *Amaranthus hypochondriacus*. Euphytica, 133: 171–178. https://doi.org/10.1023/A:102556492.

Coimbra S, Salema R (1997) Immunolocalization of arabinogalactan proteins in *Amaranthus hypochondriacus* L. ovules. Protoplasma 199: 75–82. https://doi.org/10.1007/BF02539808.

Costa Tura J, Mackenzie K (1990) Ovule and embryo sac development in *Malus pumila* L. cv. Cox's Orange Pippin, from dormancy to blossom. Ann Bot 66: 443–450. https://doi.org/10.1093/oxfordjournals.aob.a088046

Costa ML, Lopes AL, Amorim MI, Coimbra S (2017) Immunolocalization of AGPs and pectins in *Quercus suber* gametophytic structures. In: Schmidt A (eds) Plant Germline Development. Methods in Molecular Biology, vol 1669. Humana Press, New York, NY pp, 117–137. https://doi.org/10.1007/978-1-4939-7286-9_11.

Dardelle F, Lehner A, Ramdani Y, Bardor M, Lerouge P, Driouich A, Mollet J (2010) Biochemical and immunocytological characterizations of *Arabidopsis* pollen tube cell wall. Plant Physiol 153: 1563–1576. https://doi.org/10.1104/pp.110.158881.

Derksen J, Janssen GJ, Wolters- Arts M, Lichtscheidl I, Adlassnig W, Ovecka M, Doris F, Steer M (2011) Wall architecture with high porosity is established at the tip and maintained in growing pollen tubes of *Nicotiana tabacum*. Plant J 68: 495–506. https://doi.org/10.1111/j.1365-313X.2011.04703.x.

Dresselhaus T, Márton ML (2009) Micropylar pollen tube guidance and burst: adapted from defense mechanisms? Curr Opin Plant Biol 12: 773–780. https://doi.org/10.1016/j.pbi.2009.09.015.

Dresselhaus T, Sprunck S, Wessel GM (2016) Fertilization mechanisms in flowering plants. Curr Biol 26: R125–R139. https://doi.org/10.1016/j.cub.2015.12.032.

Endress PK (2011) Angiosperm ovules: diversity, development, evolution. Ann Bot 107: 1465–1489. https://doi.org/10.1093/aob/mcr120.

Feder N, O'brien TP (1968) Plant microtechnique: some principles and new methods. Am J Bot 55: 123–142. https://doi.org/10.1002/j.1537-2197.1968.tb06952.x.

Gawecki R, Sala K, Kurczyńska EU, Świątek P, Płachno BJ (2017) Immunodetection of some pectic, arabinogalactan proteins and hemicellulose epitopes in the micropylar transmitting tissue of apomictic dandelions (*Taraxacum*, Asteraceae, Lactuceae). Protoplasma 254: 657–668. https://doi.org/10.1007/s00709-016-0980-0

Gibbs PE (2014) Late- acting self- incompatibility–the pariah breeding system in flowering plants. New Phytol 203: 717–734. https://doi.org/10.1111/nph.12874.

Herrero M (2000) Changes in the ovary related to pollen tube guidance. Ann Bot 85: 79–85. https://doi.org/10.1006/anbo.1999.1014.

Herrero M (2001) Ovary signals for directional pollen tube growth. Sex Plant Reprod 14: 3–7. https://doi.org/10.1007/s004970100082.

Herrero M (2003) Male and female synchrony and the regulation of mating in flowering plants. Phil Trans Roy Soc B 358: 1019–1024. https://doi.org/10.1098/rstb.2003.1285.

Herrero M, Arbeloa A (1989) Influence of the pistil on pollen tube kinetics in peach (*Prunus persica*). Am J Bot 76: 1441–1447. https://doi.org/10.2307/2444430.

Herrero M, Dickinson HG (1979) Pollen–pistil incompatibility in *Petunia hybrida*: changes in the pistil following compatible and incompatible intraspecific crosses. J Cell Sci 36: 1–18.

Herrero M, Dickinson HG (1981) Pollen tube development in *Petunia hybrida* following compatible and incompatible intraspecific matings. J Cell Sci 47: 365–383.

Herrero M, Gascón M (1987) Prolongation of embryo sac viability in pear (*Pyrus communis*) following pollination or treatment with gibberellic acid. Ann Bot 60: 287–293.

Higashiyama T, Hamamura Y (2008) Gametophytic pollen tube guidance. Sex Plant Reprod 21: 17–26. https://doi.org/10.1007/s00497-007-0064-6.

Higashiyama T, Yabe S, Sasaki N, Nishimura Y, Miyagishima S, Kuroiwa H, Kuroiwa T (2001) Pollen tube attraction by the synergid cell. Science 293: 1480–1483.

Hofmeister W (1849) Die Entstehung des Embryos der Phanerogamen. Leipzig: Hofmeister.

Hughes J, McCully ME (1975) The use of an optical brightener in the study of plant structure. Stain Technol 50: 319. https://doi.org/10.3109/10520297509117082.

Hülskamp M, Schneitz K, Pruitt RE (1995) Genetic evidence for a long-range activity that directs pollen tube guidance in *Arabidopsis*. Plant Cell 7: 57– 64. https://doi.org/10.1105/tpc.7.1.57.

Jefferies CJ, Belcher AR (1974) A fluorescent brightener used for pollen tube identification in vivo. Stain Technol 49: 199–202.

Johansen DA (1940) Plant microtechnique. McGraw-Hill Book, New York, New York, USA.

Johnson MA, Preuss D (2002) Plotting a course: multiple signals guide pollen tubes to their targets. Dev Cell 2: 273–281. https://doi.org/10.1016/S1534-5807(02)00130-2.

Jauh G, Lord E (1996) Localization of pectins and arabinogalactan-proteins in lily (*Lilium longiflorum* L.) pollen tube and style, and their possible roles in pollination. Planta 199: 251–261. https://doi.org/10.1007/BF00196566.

Kanaoka MM (2018) Cell–cell communications and molecular mechanisms in plant sexual reproduction. J Plant Res 131: 37–47. https://doi.org/10.1007/s10265-017-0997-2.

Kasahara RD, Portereiko MF, Sandaklie-Nikolova L, Rabiger DS, Drews GN (2005) MYB98 is required for pollen tube guidance and synergid cell differentiation in *Arabidopsis*. Plant Cell, 17: 2981–2992. https://doi.org/10.1105/tpc.105.034603.

Kessler SA, Grossniklaus U (2011) She's the boss: signalling in pollen tube reception. Curr Op Plant Biol 14: 622–627. https://doi.org/10.1016/j.pbi.2011.07.012.

Knox JP, Linstead PJ, Cooper JP, Roberts K (1991) Developmentally regulated epitopes of cell surface arabinogalactan proteins and their relation to root tissue pattern formation. Plant J 1: 317–326. https://doi.org/10.1046/j.1365-313X.1991.t01-9-00999.x.

Leshem Y, Johnson C, Sundaresan V (2013) Pollen tube entry into the synergid cell of *Arabidopsis* is observed at a site distinct from the filiform apparatus. Plant Reprod 26: 93–99. https://doi.org/10.1007/s00497-013-0211-1.

Leszczuk A, Szczuka E (2018) Arabinogalactan proteins: immunolocalization in the developing ovary of a facultative apomict *Fragaria* x *ananassa* (Duch.). Plant Physiol Bioch 123: 24–33. https://doi.org/10.1016/j.plaphy.2017.12.003.

Leszczuk A, Kozioł A, Szczuka E, Zdunek A (2019a) Analysis of AGP contribution to the dynamic assembly and mechanical properties of cell wall during pollen tube growth. Plant Science 281: 9–18. https://doi.org/10.1016/j.plantsci.2019.01.005.

Leszczuk A, Szczuka E, Zduneka A (2019b) Arabinogalactan proteins: distribution during the development of male and female gametophytes. Plant Physiol Bioch 135: 9–18. https://doi.org/10.1016/j.plaphy.2018.11.023.

Leszczuk A, Wydrych J, Szczuka E (2019c) The occurrence of calcium oxalate crystals and distribution of arabinogalactan proteins (AGPs) in ovary cells during *Fragaria* x *ananassa* (Duch.) development. J Plant Growth Regul: 1–9. https://doi.org/10.1007/s00344-018-09912-7.

Li HJ, Meng JG, Yang WC (2018) Multilayered signaling pathways for pollen tube growth and guidance. Plant Reprod 31: 31–41. https://doi.org/10.1007/s00497-018-0324-7.

Linskens HF (1975) Incompatibility in Petunia. Proc R Soc Lond B 188: 299–311. https://doi.org/10.1098/rspb.1975.0021.

Linskens HF, Esser KL (1957) Über eine spezifische anfärbung der pollenschläuche im griffel und die zahl der kallosepfropfen nach selbstung und fremdung. Naturwissenschaften 44: 16. https://doi.org/10.1007/BF00629340.

Liu J, Zhang H, Cheng Y, Kafkas S, Güney M (2014) Pistillate flower development and pollen tube growth mode during the delayed fertilization stage in Corylus heterophylla Fisch. Plant Reprod 27: 145–152. https://doi.org/10.1007/s00497-014-0248-9.

Lopes AL, Costa ML, Sobral R, Costa MM, Amorim MI, Coimbra S (2016) Arabinogalactan proteins and pectin distribution during female gametogenesis in *Quercus suber* L. Ann Bot 117: 949–961. https://doi.org/10.1093/aob/mcw019.

Lopez R, Renzaglia A (2016) Arabinogalactan proteins and arabinan pectins abound in the specialized matrices surrounding female gametes of the fern *Ceratopteris richardii*. Planta 243: 947–957. https://doi.org/10.1007/s00425-015-2448-4.

Lora J, Hormaza JI, Herrero M (2016) The diversity of the pollen tube pathway in plants: toward an increasing control by the sporophyte. Front Plant Sci 7:107. https://doi.org/ 10.3389/fpls.2016.00107.

Lora J, Laux T, Hormaza JI (2018) The role of the integuments in pollen tube guidance in flowering plants. New Phytol. https://doi.org/10.1111/nph.15420.

Losada JM, Herrero M (2012) Arabinogalactan-protein secretion is associated with the acquisition of stigmatic receptivity in the apple flower. Ann Bot 110: 573–584. https://doi.org/10.1093/aob/mcs116.

Losada JM, Herrero M (2014) Glycoprotein composition along the pistil of *Malus* x *domestica* and the modulation of pollen tube growth. BMC Plant Biol 14: 1. https://doi.org/10.1186/1471-2229-14-1.

Losada JM, Herrero M (2017) Pollen tube access to the ovule is mediated by glycoprotein secretion on the obturator of apple (*Malus× domestica*, Borkh). Ann Bot 119: 989–1000. https://doi.org/10.1093/aob/mcw276.

Losada JM, Hormaza JI, Lora J (2017) Pollen-pistil interaction in pawpaw (*Asimina triloba* L.), the northernmost species of the mainly tropical family Annonaceae. Am J Bot 104:1891–1903. https://doi.org. 10.3732/ajb.1700319.

Márton ML, Cordts S, Broadhvest J, Dresselhaus T (2005) Micropylar pollen tube guidance by egg apparatus 1 of maize. Science. 307: 573–576. https://doi.org/10.1126/science.1104954.

Márton ML, Dresselhaus T (2010) Female gametophyte-controlled pollen tube guidance. Bioch Soc Trans 38: 627–30. https://doi.org/10.1042/BST0380627.

Márton ML, Fastner A, Uebler S, Dresselhaus T (2012) Overcoming hybridization barriers by the secretion of the maize pollen tube attractant ZmEA1 from *Arabidopsis* ovules. Curr Biol 22: 1194–1198. https://doi.org/ 10.1016/j.cub.2012.04.061.

Mendes SP, Mastroberti AA, Mariath JE, Vieira RC, De Toni KL (2014) Ovule and female gametophyte development in the Bromeliaceae: an embryological study of *Pitcairnia encholirioides*. Botany 92: 883–894. https://doi.org/10.1139/cjb-2014-0114.

Mizukami AG, Inatsugi R, Jiao J, et al. (2016) The AMOR arabinogalactan sugar chain induces pollen-tube competency to respond to ovular guidance. Curr Biol 26: 1091–1097.

Mizuta Y, Higashiyama T (2018) Chemical signalling for pollen tube guidance at a glance. J Cell Sci 131:208447. https://doi.org/10.1242/jcs.208447.

Mollet JC, Kim S, Jauh GY, Lord EM (2002) Arabinogalactan proteins, pollen tube growth, and the reversible effects of Yariv phenylglycoside. Protoplasma 219: 89–98. https://doi.org/10.1007/s007090200009.

Moore JP, Nguema-Ona EE, Vicré-Gibouin M Sørensen I, Willats WG, Driouich A, Farrant JM (2013) Arabinose-rich polymers as an evolutionary strategy to plasticize resurrection plant cell walls against desiccation. Planta 237: 739–754. https://doi.org/10.1007/s00425-012-1785-9.

Nguema-Ona E, Coimbra S, Vicré-Gibouin M, Mollet JC, Driouich A (2012) Arabinogalactan proteins in root and pollen-tube cells: distribution and functional aspects. Ann Bot 110: 383–404. https://doi.org/10.1093/aob/mcs143.

Okuda S, Tsutsui H, Shiina K, Sprunck S, Takeuchi H, Yui R, et al. (2009) Defensin-like polypeptide LUREs are pollen tube attractants secreted from synergid cells. Nature 458: 357–361.https://doi.org/10.1038/nature07882.

Pennell RI, Janniche L, Kjellbom P, Scofield GN, Peart JM, Roberts K (1991) Developmental regulation of a plasma membrane arabinogalactan protein epitope in oilseed rape flowers. Plant Cell 3: 1317–1326. https://doi.org/10.1105/tpc.3.12.1317.

Pereira AM, Lopes AL, Coimbra S (2016) Arabinogalactan proteins as interactors along the crosstalk between the pollen tube and the female tissues. Front Plant Sci 7: 1895. https://doi.org/ 10.3389/fpls.2016.01895.

Pereira AM, Masiero S, Nobre MS, et al. (2014) Differential expression patterns of arabinogalactan proteins in *Arabidopsis thaliana* reproductive tissues. J Exp Bot 65: 5459–5471. https://doi.org/10.1093/jxb/eru300.

Pereira LG, Coimbra S, Oliveira H, Monteiro L, Sottomayor M (2006) Expression of arabinogalactan protein genes in pollen tubes of *Arabidopsis thaliana*. Planta 223: 374–380. https://doi.org/10.1007/s00425-005-0137-4.

Pereira A, Pereira L, Coimbra S (2015) Arabinogalactan proteins: rising attention from plant biologists. Plant Reprod 28: 1–15. https://doi.org/ 10.1007/s00497-015-0254-6.

Pérez-Pérez Y, Carneros E, Berenguer E, Solís MT, Bárány I, Pintos, B, Gómez-Garay A, Risueño MC, Testillano PS (2018) Pectin de-methylesterification and AGP increase promote cell wall remodeling and are required during somatic embryogenesis of *Quercus suber*. Frontiers in plant science, 9: 1915. https://doi.org/10.3389/fpls.2018.01915.

Punwani JA, Drews GN (2008) Development and function of the synergid cell. Sex Plant Reprod 21:7–15 https://doi.org/10.1007/s00497-007-0059-3.

Punwani JA, Rabiger DS, Drews GN (2007) MYB98 positively regulates a battery of synergid-expressed genes encoding filiform apparatus–localized proteins. Plant Cell 19: 2557–2568. https://doi.org/ 10.1105/tpc.107.052076.

Sandaklie-Nikolova L, Palanivelu R, King EJ, Copenhaver GP, Drews GN (2007) Synergid cell death in *Arabidopsis* is triggered following direct interaction with the pollen tube. Plant Physiol 144: 1753–1762. https://doi.org/10.1104/pp.107.098236.

Sankaranarayanan S, Higashiyama T (2018) Capacitation in plant and animal fertilization. Trends Plant Sci 23: 129–139. https://doi.org/10.1016/j.tplants.2017.10.006.

Speranza A, Taddei AR, Gambellini G, Ovidi E, Scoccianti V (2009) The cell wall of kiwifruit pollen tubes is a target for chromium toxicity: alterations to morphology, callose pattern and arabinogalactan protein distribution. Plant Biol 11: 179–193. https://doi.org/ 10.1111/j.1438-8677.2008.00129.x.

Qin Y, Chen D, Zhao J (2007) Localization of arabinogalactan proteins in anther, pollen, and pollen tube of *Nicotiana tabacum* L. Protoplasma 231: 43–53. https://doi.org/10.1007/s00709-007-0245-z.

Sogo A, Tobe H (2006) Delayed fertilization and pollen-tube growth in pistils of *Fagus japonica* (Fagaceae). Am J Bo 93: 1748–1756. https://doi.org/10.3732/ajb.93.12.1748.

Sogo A, Tobe H (2008) Mode of pollen tube growth in pistils of *Ticodendron incognitum* (Ticodendraceae, Fagales) and the evolution of chalazogamy. Bot J Linn Soc 157: 621– 631. https://doi.org/10.1111/j.1095-8339.2008.00807.x.

Solís MT, Pintos T, Prado MJ, et al (2008) Early markers of in vitro microspore reprogramming to embryogenesis in olive (*Olea europaea* L.). Plant Sci 174: 597–605. https://doi.org/ 10.1016/j.plantsci.2008.03.014.

Su, S. and Higashiyama, T (2018) Arabinogalactan proteins and their sugar chains: functions in plant reproduction, research methods, and biosynthesis. Plant Reprod 31: 67– 75. https://doi.org/10.1007/s00497-018-0329-2.

Suárez C, Zienkiewicz A, Castro A, Zienkiewicz K, Majewska-Sawka A, Rodríguez-García, M (2013) Cellular localization and levels of pectins and arabinogalactan proteins in olive (*Olea europaea* L.) pistil tissues during development: implications for pollen–pistil interaction. Planta 237: 305–319. https://doi.org/10.1007/s00425-012-1774-z.

Vaughn KC, Talbot MJ, Offler CE, McCurdy DW (2007) Wall ingrowths in epidermal transfer cells of *Vicia faba* cotyledons are modified primary walls marked by localized accumulations of arabinogalactan proteins. Plant Cell Physiol 48: 159–168. https://doi.org/10.1093/pcp/pcl047.

Yariv J, Lis H, Katchalski E (1967) Precipitation of arabic acid and some seed polysaccharides by glycosylphenylazo dyes. Bioch J 105: 1C–2C.

Zhong J, Ren Y, Yu M, Ma T, Zhang X, Zhao J (2011) Roles of arabinogalactan proteins in cotyledon formation and cell wall deposition during embryo development of *Arabidopsis*. Protoplasma 248: 551–563. https://doi.org/10.1007/s00709-010-0204-y.

Figure legends

Fig. 1. Pollen tube arrival to the anatropous ovules of apple. Schematic representation of the pollen tube (red), reaching the different ovule structures. Bars (Y axis) show the percentage of ovary locules with pollen tubes at these structures, during the days following pollination. Each data is based on observations of three flowers/30 ovules.

Fig. 2. Pollen tube pathway in the apple ovule. A. Pollen tube (fluorescent green, red arrows) traversing the micropyle, flanked by the inner integuments six days after pollination. B. Pollen tube traversing the nucellus and entering the female gametophyte, seven days after pollination. Insets show the ovule area (pink shaded square) traversed by pollen tube (red color) in the corresponding images. 10µm sections of the apple ovules embedded in paraffin and stained with aniline blue to detect callose in pollen tubes. dap, days after pollination; fg, female gametophyte; ii, inner integument; nuc, nucellus; obt, obturator; oi, outer integument; pt, pollen tube. Scale bars: 50µm.

Fig. 3. Detection of AGP secretions in apple ovules. A. Area of the ovule (pink shaded square) represented in B-D. B. Fresh ovule at anthesis showing the micropyle with the negative control α-Galactosyl-Yariv reagent. C. Same area revealing an AGP-rich secretion from the micropyle (arrows). D. Whole mount of the ovule from pollinated flowers showing a pollen tube entering the micropylar area. E. Area of the ovule (pink shaded square) imaged in F-H. F. Dissected nucellus (integuments removed), stained with the negative control α-Galactosyl-Yariv reagent. G. Nucellus with a droplet secretion at the tip containing AGPs. H. Pollen tube entrance in the nucellus. Whole mounts of *in vivo* ovules tested with the negative control α-Galactosyl-Yariv reagent (B and F), or with β-Glucosyl-Yariv reagent positive for AGPs (C and G). ii: inner integument, nu: nucellus, obt: obturator, oi: outer integument; pt, pollen tube. Scale bars: 20µm.

Fig. 4. Immunolocalization of AGPs in the ovules along the pollen tube pathway. A. Nucellar tip facing the micropyle at anthesis (0 daa). B. Immunolocalization of the exudate from the nucellus rich in JIM13 AGP epitopes (white arrows). C. Merged images. D. Pollen tube growth in the micropyle six days after pollination (6 dap). E. AGP epitopes recoginized by the JIM 13 mAb along the micropylar canal

(white arrows). F. Merged images. G. Pollen tubes (red arrows) in the area between the nucellus tip and the inner integuments. H. Same section immunolocalized with the JIM13 mAb showing weakening of epitope signaling in the area of the exudate. I. Merged images. Insets show the schematic representation of the apple ovules highlighting the pollen tube elongation in red, and the areas shown by the photographs, pink shaded. 2µm sections of ovules stained with calcofluor white (calc: A,D,G) that stains cellulose of the cell walls in blue; immunolocalized with JIM13 mAb and detected with Alexa 488 anti-Rat secondary antibody conjugated with FITC that shows a green color (B,E,H), and counterstained with calcofluor white (C,F,I); daa, days after anthesis; dap, days after pollination; ii, inner integument; nu, nucellus; pt, pollen tube. Scale bars: 20µm.

Fig. 5. AGPs in the nucellus of apple ovules before and after pollen tube penetration. A. Glycoproteins (white arrows) in the surface of a row of nucellar cells leading to the egg apparatus, at anthesis (0 daa). B. At the time of pollen tube penetration and fertilization, these glycoproteins vanish from the areas of pollen tube growth (red arrows). C. AGP epitopes (white arrows) accumulate in the nucellus of unpollinated flowers six days after anthesis (6 daa). 2µm sections of ovules immunolocalized with JIM8 mAb and detected with an Alexa 488 anti-Rat secondary antibody conjugated with FITC that shows a green color. daa, days after anthesis; dap, days after pollination; es, embryo sac; ii, inner integument; nu, nucellus; pt, pollen tube. Scale bars: 20µm.

Fig. 6. Changes in the apple female gametophyte. A. Female gametophyte at anthesis (0 daa) with two synergids, egg cell, and two polar nuclei. B. Female gametophyte six days after pollination (6 dap), showing the egg cell, unfused polar nuclei, and starch in the central cell. C. Unfertilized female gametophyte six days after anthesis (6 daa), with fused polar nuclei. D. Fertilized ovule, nine days after pollination (9 dap), with an elongated embryo sac, and endosperm nuclei. E-H. Details of the synergids, with filiform apparatus (arrowheads) strongly stained for insoluble carbohydrates at the stages represented in the images above. E. Synergids with a conspicuous vacuole and a developing filiform apparatus, at anthesis (0 daa). F. Fully mature filiform apparatus at the time of fertilization (6 dap), and one synergid

degenerating (darker blue cytoplasm). G. Filiform apparatus of an unfertilized embryo sac (6 daa). H. Collapsed filiform apparatus in a fertilized embryo sac (9 dap), with vanishing polysaccharides. 2µm sections of ovules stained with periodic-acid-Shiffs reagent for insoluble polysaccharides and counterstained with toluidine blue for general cell structure. daa, days after anthesis; dap, days after pollination; ec, egg cell; en, endosperm nuclei; pn, polar nuclei; syn, synergids; zyg: zygote. A-D scale bars: 20µm; E-H scale bars: 10µm.

Fig. 7. Changes in AGPs in the embryo sac with fertilization. A. The female gametophyte at anthesis (0 daa) with young synergids. B. The primary wall of the synergids, and the convoluted wall of the central cell strongly stains for AGPs (white arrows). C. Merged images. D. Female gametophyte at the time of fertilization six days after pollination (6 dap). E. Glycoproteins strongly labelled the elongated wall of the central cell, as well as the primarly wall of the egg cell, and vesicles in the central cell (white arrows). F. Merged images. G. Unpollinated female gametophyte six days after anthesis (6 daa). H. The unfertilized female gametophyte contains numerous vesicles that label intensely for AGPs (arrowheads). I. Merged images. 2µm sections of ovules stained with DAPI for DNA in nuclei in light blue (A, D, G), immunolocalized with JIM13 mAb and detected with an Alexa 488 anti-Rat secondary antibody conjugated with FITC that shows a green color (B, E, H), and counterstained with DAPI for DNA in nuclei in light blue (C, F, I). cc, central cell; daa, days after anthesis; dap, days after pollination; ec, egg cell; syn, synergids. Scale bars: 20 µm.

Fig. 8. Arabinogalactans in the egg apparatus, zygote and embryo in apple. A. Cellulose of the convoluted walls of the filiform apparatus three days after pollination (3 dap). B. AGPs epitopes localized in the filiform apparatus cell walls (white arrows). C. Merged images. D. Expanded filiform apparatus before pollen tube arrival, five days after pollination (5 dap). E. At this time, AGPs profusely labeled the walls of the filiform apparatus (white arrows). F. Merged images. G. Collapsed filiform apparatus of a fertilized embryo sac, seven days after pollination (7 dap). H. AGPs label the primary cell wall of the zygote (arrows). I. Merged images. J. Lack of a filiform apparatus in a fertilized embryo sac, nine days

after pollination (9 dap). K. AGPs in the primary walls of the young embryo (white arrows). L. Merged images. 2µm sections of ovules stained with calcofluor white (calc) that stains cellulose of the cell walls in blue (A, D, G, J), immunolocalized with JIM13 mAb and detected with an Alexa 488 anti-rat secondary antibody conjugated with FITC that shows a green color (B, E, H, K), and counterstained with calcofluor white (C, F, I, L). daa, days after anthesis; dap, dasys after pollination; emb, embryo; zyg, zygote. Scale bars: 10µm.

Fig. 9. Primary and secondary cell wall composition in the apple embryo sac. Schematic drawings of the embryo sac before and after fertilization, showing the localization of cellulose (purple) indicative of secondary cell wall formation, and arabinogalactan proteins (green), indicative of primary cell wall composition. From left to right: fully formed female gametophyte at anthesis; pollen tube penetration (grey) in the embryo sac; fertilization with zygote and endosperm; cellular embryo and endosperm. In all developmental stages, AGP-rich primary cell walls separate the functional domains of the embryo sac. cc, central cell; ec, egg cell; emb, embryo; en, endosperm; syn, synergid; zyg, zygoge.

Supplementary Fig. 1. AGPs labelled with JIM13 mAb in the nucellus of apple ovules before and after pollen tube penetration. A. Glycoprotein epitopes in the surface of a row of cells leading to the egg apparatus (white arrows), at anthesis (0 daa). B. At the time of pollen tube penetration and fertilization, these glycoproteins vanish from the areas of pollen tube growth. 2µm sections of ovules immunolocalized with JIM13 mAb and detected with an Alexa 488 anti-Rat secondary antibody conjugated with FITC that shows a green color. Daa, days after anthesis; dap, days after pollination; nu, nucellus; pt, pollen tube. Scale bars: 20µm.

Supplementary Fig. 2. Changes in the filiform apparatus of the synergids during the post pollination stages in apple. A. While the embryo sac accumulates starch, the filiform apparatus of the synergids (black arrows) shows accumulation of polysaccharides three days after pollination (3 dap). B. Concomitant with pollen tube arrival, one synergid degenerates (black arrow). C. Following fertilization, upon zygote formation, the filiform apparatus (black arrows) degenerates, losing polysaccharide staining.

2µm sections of ovules stained with periodic acid Shiffs – PAS for insoluble polysaccharides (pink to purple color). Dap, days after pollination; es, embryo sac; fa, filiform apparatus; pt, pollen tube; syn, synergid; zyg, zygote. Scale bars: 20µm.

Figure legends

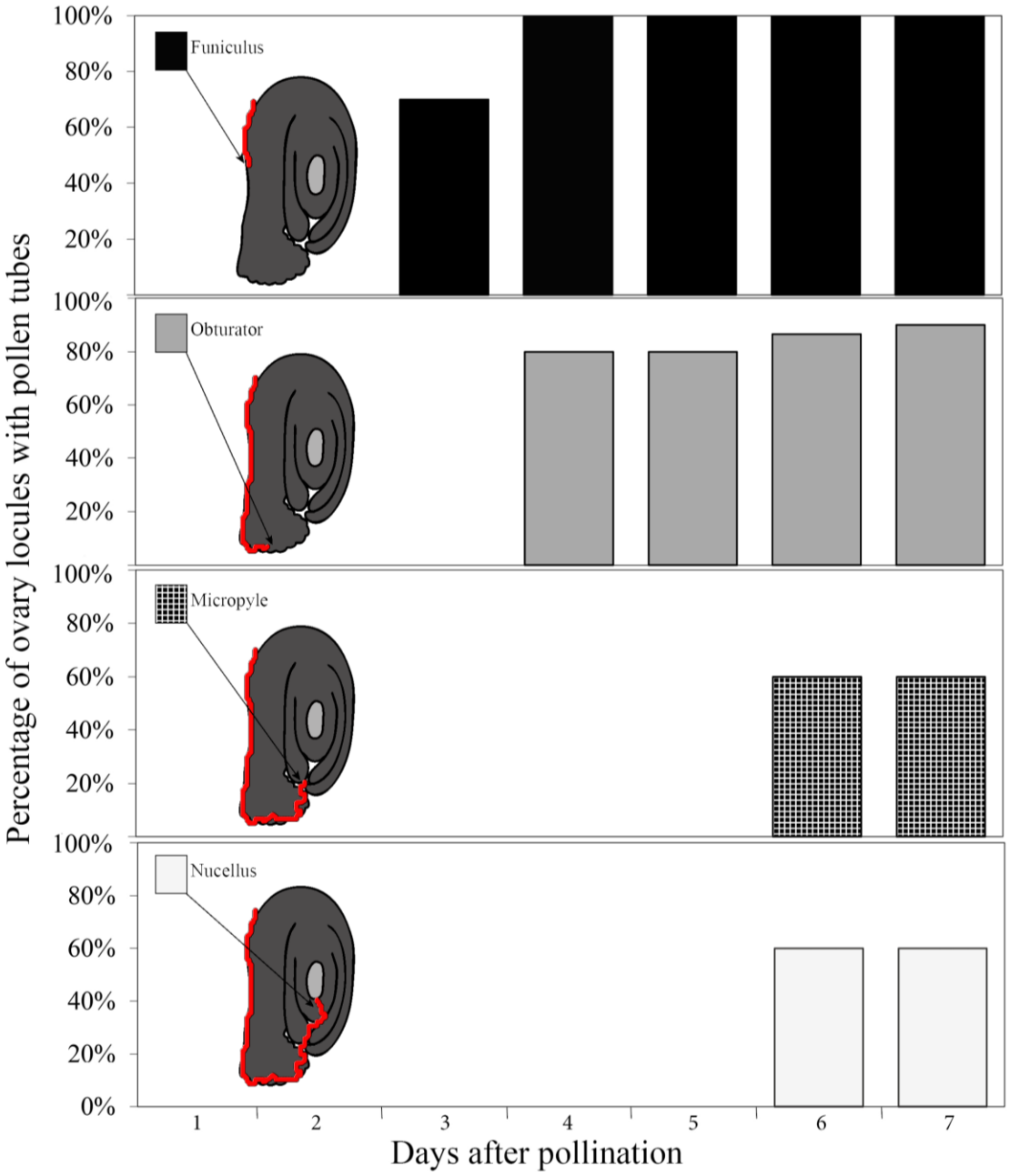

Fig. 1. Pollen tube arrival to the anatropous ovules of apple. Schematic representation of the pollen tube (red), reaching the different ovule structures. Bars (Y axis) show the percentage of ovary locules with pollen tubes at these structures, during the days following pollination.

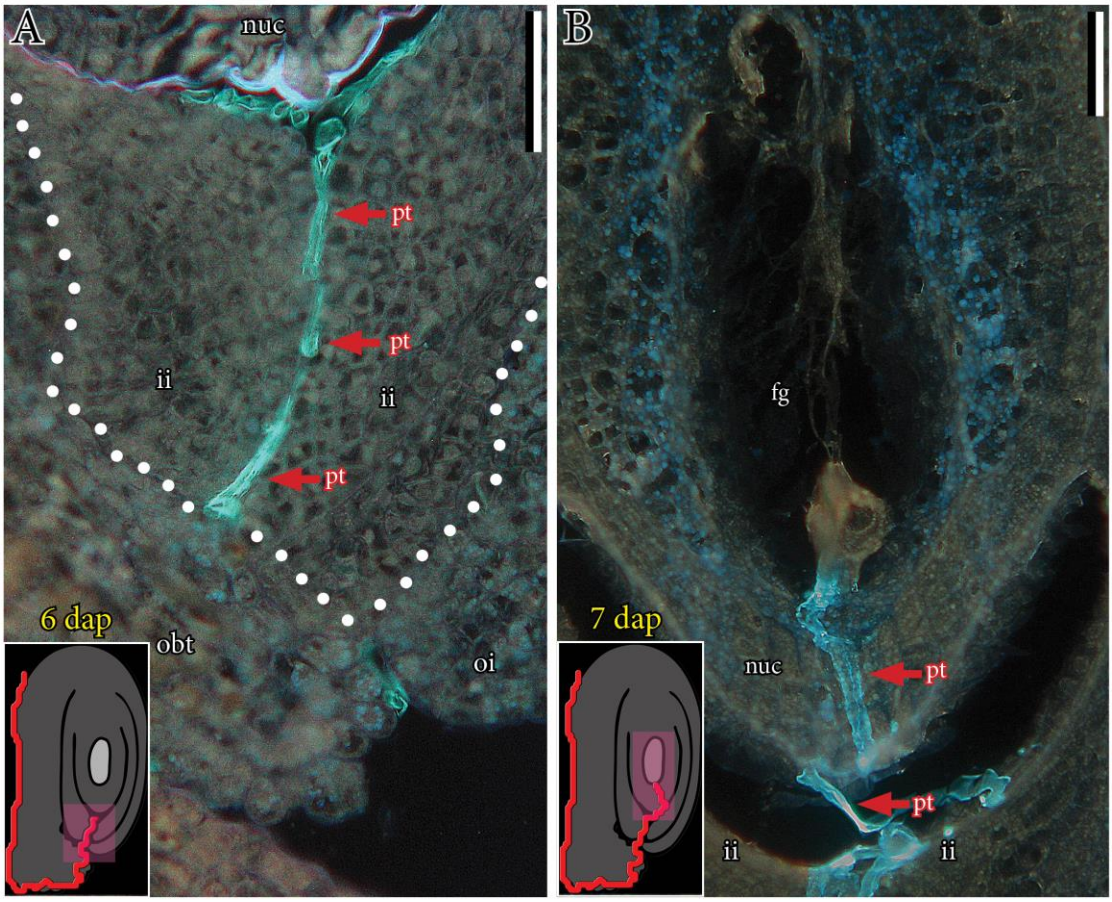

Fig. 2. Pollen tube pathway in the apple ovule. A. Pollen tube (fluorescent green, red arrows) traversing the micropyle, flanked by the inner integuments six days after pollination. B. Pollen tube traversing the nucellus and entering the female gametophyte, seven days after pollination. Insets show the ovule area (pink shaded square) traversed by pollen tube (red color) in the corresponding images. 10µm sections of the apple ovules embedded in paraffin and stained with aniline blue to detect callose in pollen tubes. dap, days after pollination; fg, female gametophyte; nuc, nucellus; ii, inner integument; obt, obturator; oi, outer integument; pt, pollen tube. Scale bars: 50µm.

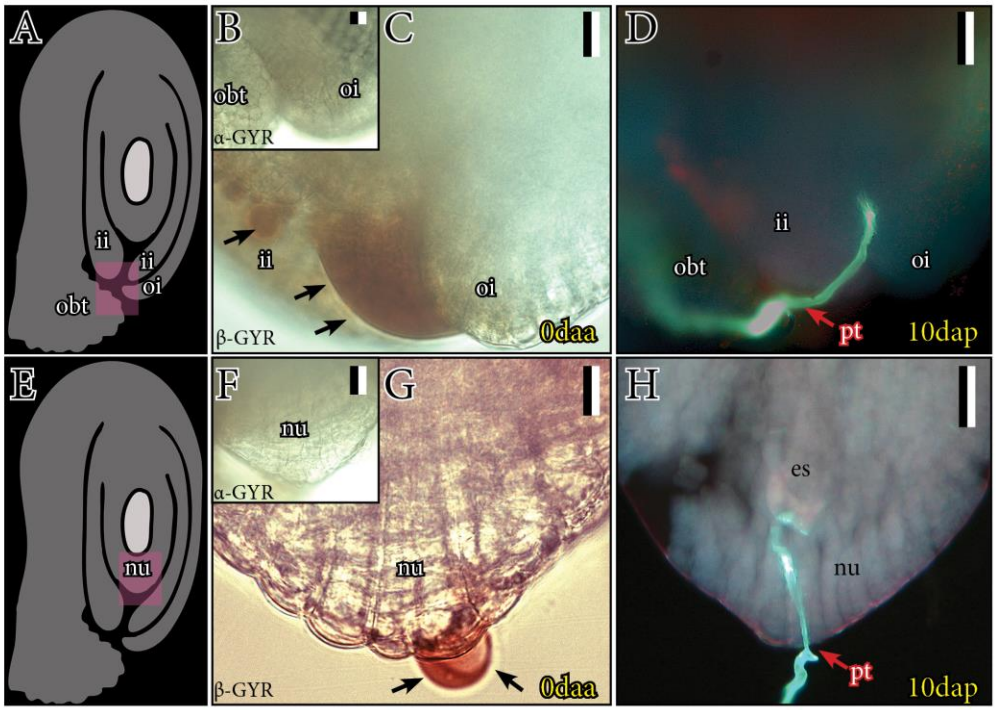

Fig. 3. Detection of AGP secretions in apple ovules. A. Area of the ovule (pink shaded square) represented in B and C. B. Fresh ovule at anthesis showing the micropyle with the negative control α-Galactosyl-Yariv reagent. C. Same area revealing an AGP-rich secretion from the micropyle (arrows). D. Whole mount of the ovule from pollinated flowers showing a pollen tube entering the micropylar area. E. Area of the ovule (pink shaded square) imaged in F,G, and H. F. Dissected nucellus (integuments removed), stained with the negative control α-Galactosyl-Yariv reagent. G. Nucellus with a droplet secretion at the tip containing AGPs. H. Pollen tube entrance in the nucellus. Whole mounts of *in vivo* ovules tested with the negative control α-Galactosyl-Yariv reagent (B and F), or with β-Glucosyl-Yariv reagent positive for AGPs (C and G). ii: inner integument, nu: nucellus, obt: obturator, oi: outer integument; pt, pollen tube. Scale bars: 20µm.

1

2

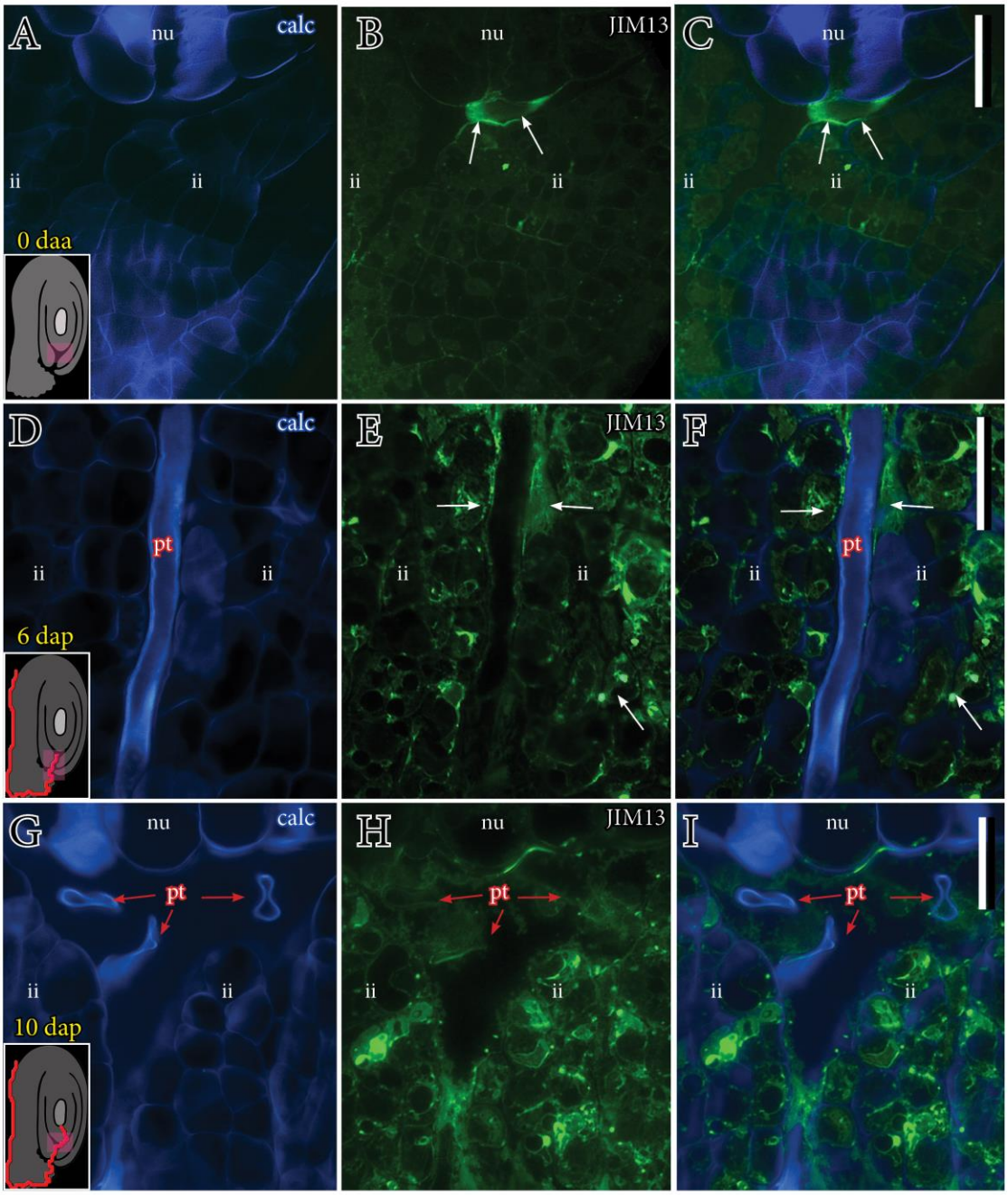
A
nu
calc
ii
ii
0 daa
B
nu
JIM13
ii
ii
C
nu
ii
ii
D
calc
pt
ii
ii
6 dap
E
JIM13
ii
ii
F
pt
ii
ii
G
nu
calc
pt
ii
ii
10 dap
H
nu
JIM13
pt
ii
ii
I
nu
pt
ii
ii

3

Fig. 4. Immunolocalization of AGPs in the ovules along the pollen tube pathway. A. Nucellar tip facing the micropyle at anthesis (0daa). B. Immunolocaliation of the exudate from the nucellus rich in JIM13 AGP epitopes (white arrows). C. Merged images. D. Pollen tube growth in the micropyle six days after pollination (6 dap). E. AGP epitopes recoginized by the JIM 13 mAb along the micropylar canal (white arrows). F. Merged images. G. Pollen tubes (red arrows) in the area between the nucellus tip and the inner integuments. H. Same section immunolocalized with the JIM13 mAb showing weakening of epitope signaling in the area of the exudate. I. Merged images. Insets show the schematic representation of the apple ovules highlighting in red the pollen tube elongation and the areas shown by the photographs pink shaded. 2µm sections of ovules immunolocalized with JIM13 mAb and detected with Alexa 488 anti-Rat secondary antibody conjugated with FITC that shows a green color (B,E,H), and counterstained with calcofluor white (calc: A,D,G) that stains cellulose of the cell walls in blue; daa, days after anthesis; dap, days after pollination; ii, inner integument; nu, nucellus; pt, pollen tube. Scale bars: 20µm.

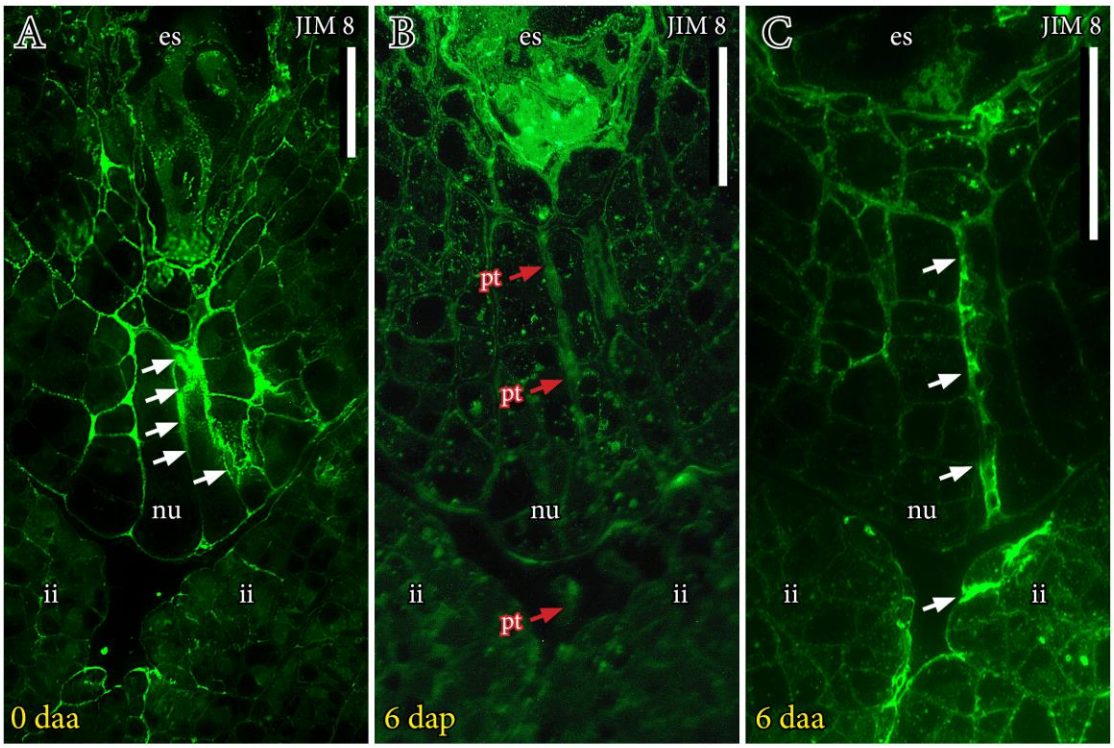

Fig. 5. AGPs in the nucellus of apple ovules before and after pollen tube penetration. A. Glycoproteins (white arrows) in the surface of a row of nucellar cells leading to the egg apparatus, at anthesis (0 daa). B. At the time of pollen tube penetration and fertilization, these glycoproteins vanish from the areas of pollen tube growth (red arrows). C. AGP epitopes (white arrows) accumulate in the nucellus of unpollinated flowers six days after anthesis (6daa). 2µm sections of ovules immunolocalized with JIM8 mAb and detected with an Alexa 488 anti-Rat secondary antibody conjugated with FITC that shows a green color. daa, days after anthesis; dap, days after pollination; es, embryo sac; ii, inner integument; nu, nucellus; pt, pollen tube. Scale bars: 20µm.

Fig. 6. Changes in the apple female gametophyte. A. Female gametophyte at anthesis (0daa) with two synergids, egg cell, and two polar nuclei. B. Female gametophyte six days after pollination (6dap), showing the egg cell, unfused polar nuclei, and starch in the central cell. C. Unfertilized female gametophyte six days after anthesis (6daa), with fused polar nuclei. D. Fertilized ovule, nine days after pollination (9dap), with an elongated embryo sac, and endosperm nuclei. E-H. Details of the synergids, with filiform apparatus (arrowheads) strongly stained for insoluble carbohydrates at the stages represented in the images above. E. Synergids with a conspicuous vacuole and a developing filiform apparatus, at anthesis (0daa). F. Fully mature filiform apparatus at the time of fertilization (6dap), and one synergid degenerating (darker blue cytoplasm). G. Filiform apparatus of an unfertilized embryo sac (6daa). H. Collapsed filiform apparatus in a fertilized embryo sac (9dap), with vanishing polysaccharides. 2µm sections of ovules stained with periodic-acid-Shiffs reagent for insoluble polysaccharides and counterstained with toluidine blue for general cell structure. daa, days after anthesis; dap, days after pollination; ec, egg cell; en, endosperm nuclei; pn, polar nuclei; syn, synergids; zyg: zygote. A-D scale bars: 20µm; E-H scale bars: 10µm.

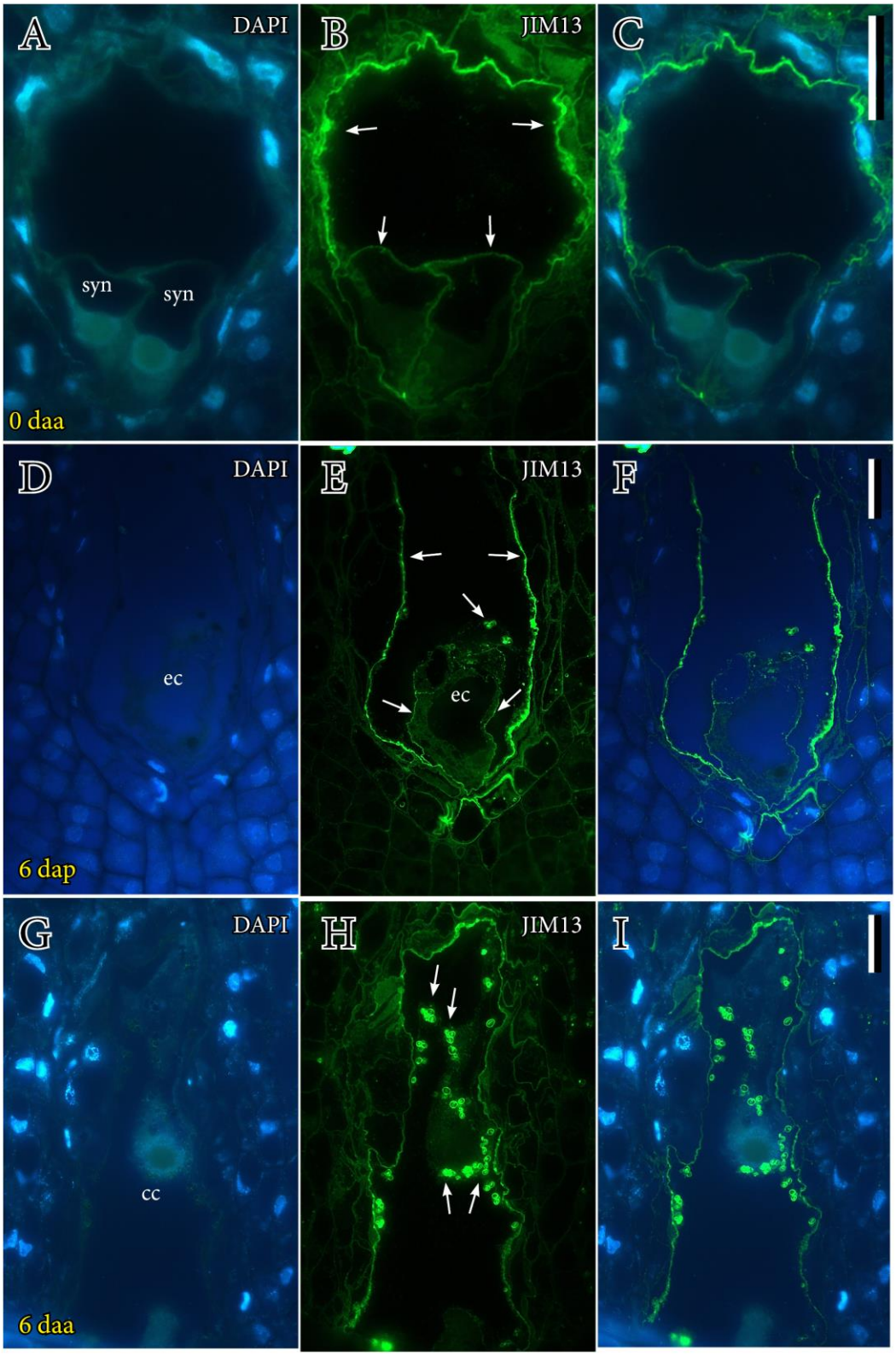
A
DAPI
syn
syn
0 daa
B
JIM13
C
D
DAPI
ec
6 dap
E
JIM13
ec
F
G
DAPI
cc
6 daa
H
JIM13
I

1

Fig. 7. Changes in AGPs in the embryo sac with fertilization. A. The female gametophyte at anthesis (0daa) with young synergids. B. The primary wall of the synergids, and the convoluted wall of the central cell strongly stains for AGPs (white arrows). C. Merged images. D. Female gametophyte at the time of fertilization six days after pollination (6dap). E. Glycoproteins strongly labelled the elongated wall of the central cell, as well as the primarly wall of the egg cell, and vesicles in the central cell (white arrows). F. Merged images. G. Unpollinated female gametophyte six days after anthesis (6daa). H. The unfertilized female gametophyte contains numerous vesicles that label intensely for AGPs (arrowheads). I. Merged images. 2µm sections of ovules stained with DAPI for DNA in nuclei in light blue (A, D, G), immunolocalized with JIM13 mAb and detected with an Alexa 488 anti-Rat secondary antibody conjugated with FITC that shows a green color (B, E, H), and counterstained with DAPI for DNA in nuclei in light blue (C, F, I). cc, central cell; daa, days after anthesis; dap, days after pollination; ec, egg cell; syn, synergids. Scale bars: 20 µm.

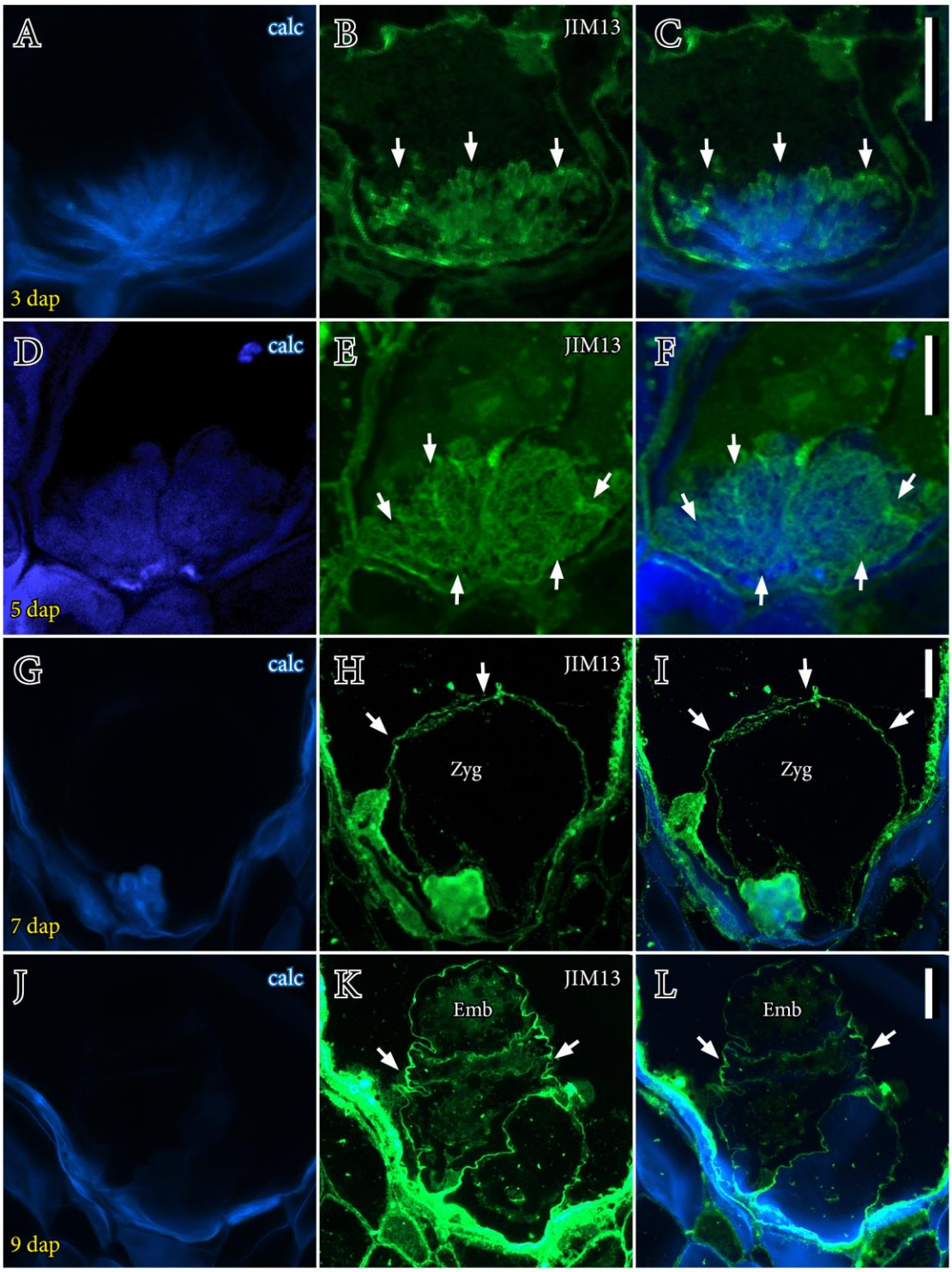
A
calc
3 dap
B
JIM13
C
D
calc
5 dap
E
JIM13
F
G
calc
7 dap
H
JIM13
Zyg
I
Zyg
J
calc
9 dap
K
JIM13
Emb
L
Emb

1

2

Fig. 8. Arabinogalactans in the egg apparatus, zygote and embryo in apple. A. Cellulose of the convoluted walls of the filiform apparatus three days after pollination (3dap). B. AGPs epitopes localized in the filiform apparatus cell walls (white arrows). C. Merged images. D. Expanded filiform apparatus before pollen tube arrival, five days after pollination (5dap). E. At this time, AGPs profusely labeled the walls of the filiform apparatus (white arrows). F. Merged images. G. Collapsed filiform apparatus of a fertilized embryo sac, seven days after pollination (7dap). H. AGPs label the primary cell wall of the zygote (arrows). I. Merged images. J. Lack of a filiform apparatus in a fertilized embryo sac, nine days after pollination (9dap). K. AGPs in the primary walls of the young embryo (white arrows). L. Merged images. 2µm sections of ovules stained with calcofluor white (calc) that stains cellulose of the cell walls in blue (A, D, G, J), immunolocalized with JIM13 mAb and detected with an Alexa 488 anti-rat secondary antibody conjugated with FITC that shows a green color (B, E, H, K), and counterstained with calcofluor white (C, F, I, L). daa, days after anthesis; dap, dasys after pollination; emb, embryo; zyg, zygote. Scale bars: 10µm.

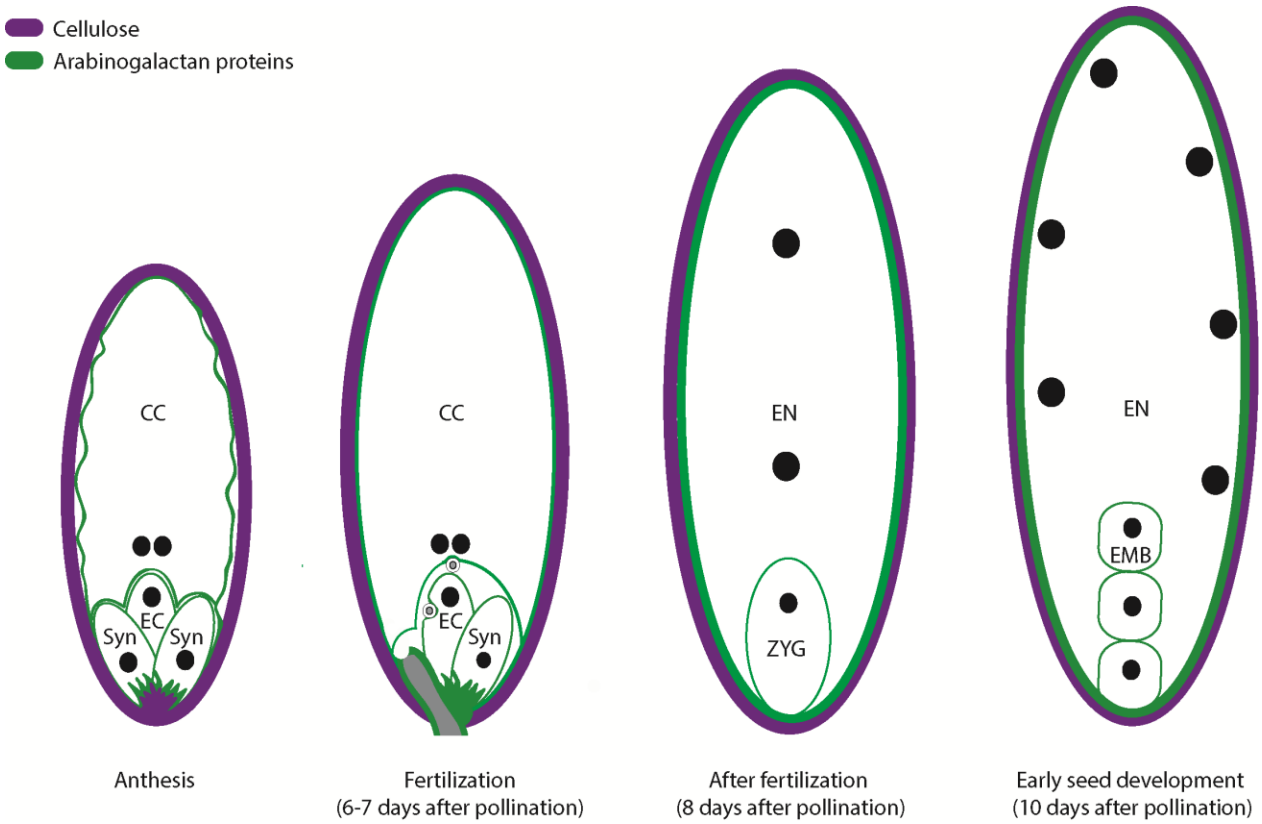

Fig. 9. Primary and secondary cell wall composition in the apple embryo sac. Schematic drawings of the embryo sac before and after fertilization, showing the localization of cellulose (purple) indicative of secondary cell wall formation, and arabinogalactan proteins (green), indicative of primary cell wall composition. From left to right: fully formed female gametophyte at anthesis; pollen tube penetration (grey) in the embryo sac; fertilization with zygote and endosperm; cellular embryo and endosperm. In all developmental stages, AGP-rich primary cell walls separate the functional domains of the embryo sac. cc, central cell; ec, egg cell; emb, embryo; en, endosperm; syn, synergid; zyg, zygoge.

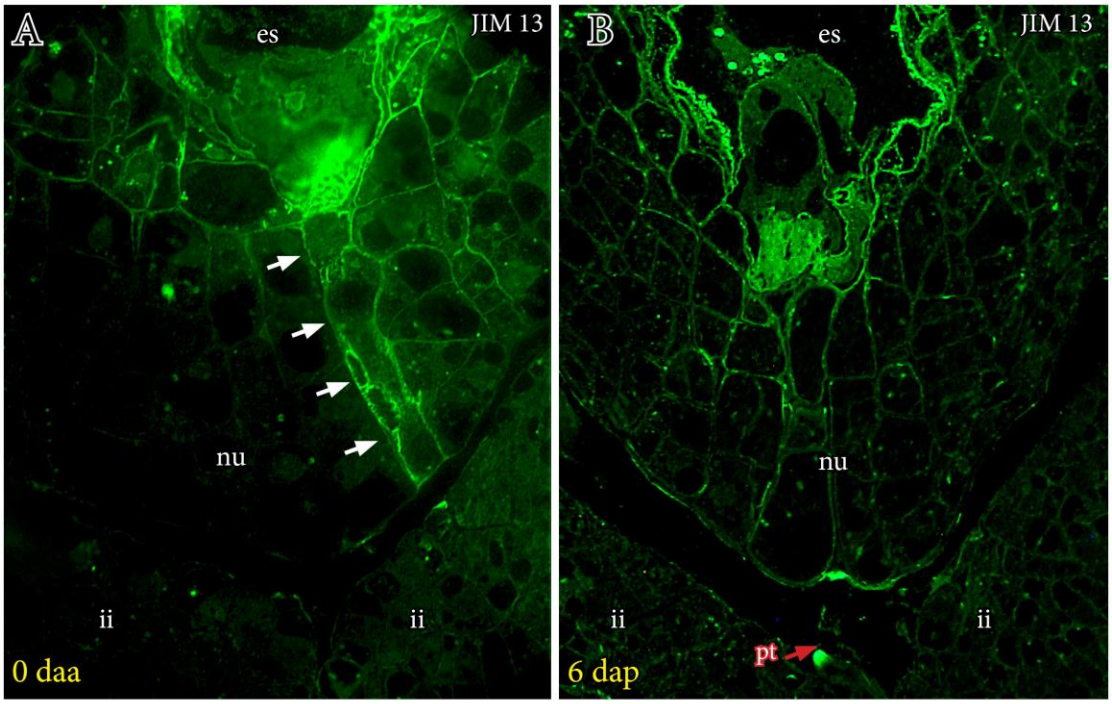

Supplementary Fig. 1. AGPs labelled with JIM13 in the nucellus of apple ovules before and after pollen tube penetration. A. Glycoproteins in the surface of a row of cells leading to the egg apparatus (white arrows), at anthesis (0daa). B. At the time of pollen tube penetration (inset) and fertilization, these glycoproteins vanish from the areas of pollen tube growth. Inset shows detail of pollen tube penetration in

the nucellus stained with calcofluor white for cellulose. 2µm sections of ovules immunolocalized with JIM13 mAb and detected with an Alexa 488 anti-Rat secondary antibody conjugated with FITC that shows a green color. Inset shows stain with calcofluor white (calc) that stains cellulose of the cell walls in blue. Daa, days after anthesis; dap, days after pollination; nu, nucellus; pt, pollen tube. Scale bars: 20µm.

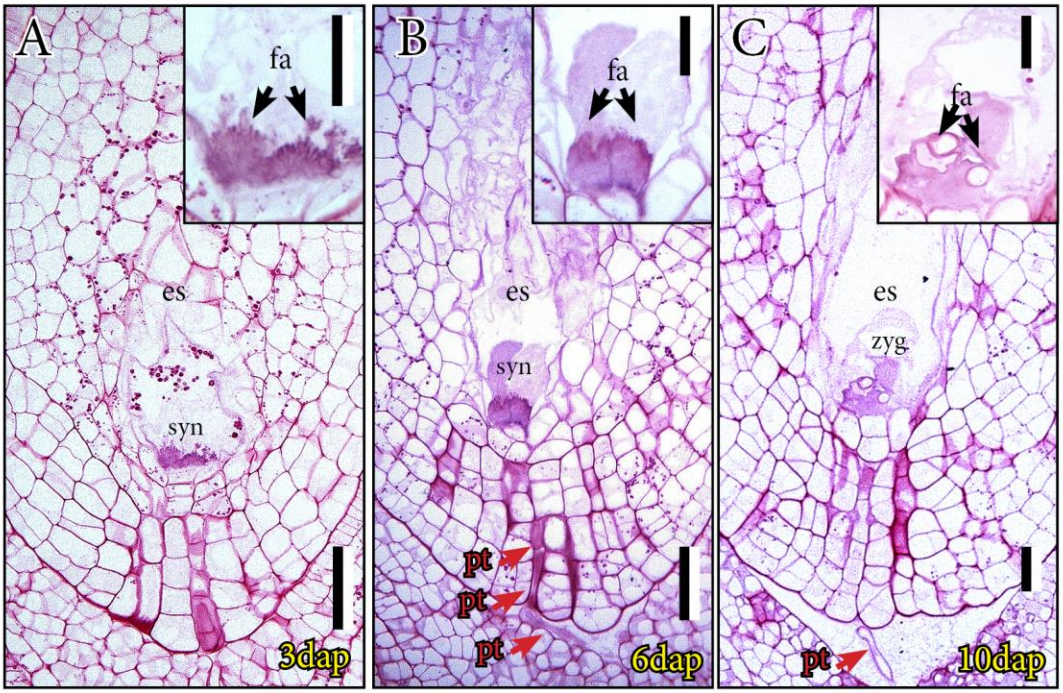

Supplementary Fig. 2. Changes in the filiform apparatus of the synergids during the post pollination stages in apple. A. While the embryo sac accumulates starch, the filiform apparatus of the synergids (black arrows) shows accumulation of polysaccharides three days after pollination (3dap). B. Concomitant with pollen tube arrival, one synergid degenerates (black arrows). D. Following fertilization, upon zygote formation, the filiform apparatus (black arrows) degenerates, losing polysaccharide staining. 2µm sections of ovules stained with periodic acid Shiffs – PAS for insoluble polysaccharides (pink to purple color). Dap, days after pollination; es, embryo sac; fa, filiform apparatus; pt, pollen tube; syn, synergid; zyg, zygote. Scale bars: 20µm.